Quantifying the CaO and CaF_2 content of industrial ladle furnace slag with optical emissions measured through the casting spout

Henri Pauna, Matti Aula, Marko Huttula, Timo Fabritius*

Dr. H. Pauna, Dr. M. Aula, Prof. T. Fabritius,
Process Metallurgy Research Unit, P.O. Box 4300, FI-90014, University of Oulu, Finland
Email Address: henri.pauna@oulu.fi
Prof. M. Huttula
Nano and Molecular Systems Research Unit, P.O. Box 3000, FI-90014, University of Oulu, Finland

Keywords: *Ladle furnace, optical emission spectroscopy, slag composition, fluorite, lime*

CaO and CaF_2 are important slag constituents and additive materials in secondary metallurgy. Optimization of the quantity of these compounds has a key role in adjusting the slag chemistry for optimal refining properties. In this study, the CaO and CaF_2 content of the slag has been analyzed with optical emissions from an industrial ladle furnace measured through the casting spout. Molecular optical emissions from CaO and CaF were observed directly from the molten bath and the arc, whereas atomic emission lines from the slag components were detected in the arc spectra. Optical emissions from CaO, CaF, and atomic calcium lines have been correlated with the CaO and CaF_2 content of the slag. The CaO and CaF_2 content of the slag could be evaluated from the spectra ranging from 10 to 41 min before the X-ray fluorescence (XRF) analysis was finished. The mean differences between the OES and XRF analysis were 0.59 % and 0.61 % for CaF_2, and 2.19 % and 0.67 % for CaO when using the spectra from the molten bath and the arc, respectively. The method has the potential to work as an *in situ* online measurement system due to real-time data acquisition and fast computation times.

1 Introduction

Industrial electric arc furnaces and ladle furnaces present a challenging environment for empirical *in situ* on-line analysis. The improvement of current practices, more flexible process control and development of new analysis methods are important research topics due to their direct effect on the efficiency of the furnace. The pivotal role of electricity-based melting in the future of more environmentally friendly steelmaking emphasizes, even more, the need for online process control.

Both lime (CaO) and fluorite (CaF_2) have a key role in secondary metallurgy. CaO is used as a common flux material to remove impurities, such as sulfur and phosphorus, from the bath [1], whereas CaF_2 is typically used to adjust the viscosity of the slag [2, 3, 4, 5, 6, 7]. There is a driving force to optimize the amount of these compounds in the steelmaking since producing CaO from

limestone causes CO_2 emissions, whereas an excessive amount of CaF_2 can increase the solubility of MgO-based refractories into the slag [8]. Consequently, the optimization of the use of CaO and CaF_2 in the steel industry is important in order to mitigate the indirect carbon footprint and increase refractory lifetime. These materials are frequently added into the furnace during the ladle process, and thus online information on the slag composition would help to adjust the quantity of the additive materials.

A conventional method to determine the slag composition on site is to perform an X-ray fluorescence (XRF) analysis, which requires sampling, sample preparation, and possibly transportation to the XRF equipment. The slag sample and its preparation can result in a composition analysis error since the point-like sample of the whole slag volume might not represent the whole slag and the quality of the slag samples may vary. With an on-line slag composition analysis solution, the error related to the sample preparation would be removed and the evolution of the slag composition could be observed in real-time. Speeding up the analysis or bringing it online would also increase material efficiency and financial savings. For example, Picon *et al.* [9] have characterized ladle furnace slags with hyperspectral reflectance after slag sampling and reached savings of 0.71 euros per ton of steel. These results are encouraging and motivating to develop an online slag composition analysis system, where the amount of impurities and valuable alloying elements could be controlled in real-time.

Optical emission spectroscopy (OES) has proven to be a potential solution for online analysis of various parameters, such as slag composition, molten bath surface temperature, and radiative heat transfer for electric arc furnaces and ladle furnaces [10, 11, 12, 13, 14, 15, 16, 17]. In this work, optical emissions of the electric arc and slag surface have been measured through the casting spout of an industrial ladle furnace. The results show that the electric arc spectra have an abundance of optical emissions from the slag components, both atomic and molecular. Furthermore, molecular optical emissions from CaO and CaF can be observed even directly from the slag surface when the arc is switched off. The optical emissions from CaO and CaF molecules together with calcium atoms have been correlated with the endpoint CaO and CaF_2 slag content. However, the casting spout has its disadvantages as a measurement location, which will be discussed in this article.

2 Methods and materials

The measurement campaign was conducted in an industrial LF at a European steel plant for carbon steel grades. The optical emissions were measured with a Czerny-Turner Avaspec-ULS2048 spectrometer covering 496.655 - 1000.000 nm with a spectral resolution of 0.151 nm. Spectra were recorded at a rate of two spectra per second. The measurement system was placed outside the furnace roughly 5 m away from the electric arcs. The measurement head was pointing towards the casting spout of the furnace. Due to this positioning of the measurement head, the measured light was not always directly from the electric arcs, but from the reflections of the arc. The purpose of choosing this position was to validate whether or not the casting spout could be used for OES measurements. Furthermore, since it could be that welding the measurement equipment to the furnace would not be an option, this measurement location enables installing the equipment outside the furnace. Whether the OES instrumentation is installed to the roof or outside the furnace, it has been observed to require only minimal maintenance that can be done at the scheduled furnace maintenance [15, 16].

After each heat, slag samples were taken from the molten bath with a sampling rod as a standard procedure of the furnace operation. The samples were prepared for on-site XRF slag composition analysis. These XRF slag compositions are used as reference data for the OES spectra. The major slag components were CaO, CaF_2, SiO_2, MgO, MnO, and Al_2O_3. The XRF slag compositions and slag component ratios have been normalized with respect to the highest values and the timestamps are in arbitrary units due to confidentiality purposes.

The data batch consists of 101 carbon steel grade heats, of which 66 had molecular optical

emissions spectra when the arc was off or not directly in the view-cone, 86 had arc spectra, and 6 had neither band nor arc spectra. During the data analysis, it was noted that choosing spectra for the correlation analysis between OES and XRF requires careful selection and clear boundary conditions for the specifics of the spectra. The spectra where the arc was off or not in the view-cone of the measurement head were characterized with thermal radiation temperature. The spectra where the arc was in the view-cone (arc spectra) have been analyzed separately from those where the arc was not in the view-cone (molten bath spectra). Only the heats with at least 60 s of consequent spectra were taken into the analysis for the spectra from the molten bath. For the spectra from the arc, only a few last spectra were used.

3 Theoretical

Electric arcs form plasma, where material from the molten bath and atmosphere dissociate into atoms and molecules. The high energy of the arc excites the particles within the plasma, causing them to radiate at wavelengths that are characteristic of each element and molecule. An atomic emission line is labeled with the element followed by ionization degree in Roman numerals and wavelength in nanometers. Roman numerals I and II refer to neutral and singly ionized atoms, respectively. The atomic emission lines and their relevant information are thoroughly listed in the NIST Atomic Spectra Database [18]. When the arc is switched off, the spectra consist of heat radiation from the molten bath and usually also atomic optical emissions from alkali atoms.

Phenomena that were observed to significantly affect especially the CaF molecular emission bands were self-absorption (SA) and self-reversal (SR). SA occurs when a photon emitted by a particle is absorbed by another particle within the plasma. This may happen e.g. if particles emit photons near the high-temperature center of the arc which are then absorbed by particles at the cooler edges of the arc. Once the photon is self-absorbed, the excited energy may be released as another photon to an arbitrary direction or via non-radiative relaxation. This phenomenon decreases the intensity of light near the vicinity of the central wavelength of the optical emission [19, 20]. SR is an extremity of SA, where the intensity near the central wavelength decreases so much that a notch is formed instead of an emission line.

The temperature was determined from the heat radiation with Planck's law for the spectra in which the arc was off or not directly in the view-cone of the measurement head. The law was fitted to the spectra, excluding the wavelength ranges where the molecular or atomic optical emissions reside. First, the law was fitted to the spectrum by taking temperatures from 100 to 3000 K in 100 K steps, from which the best fit and corresponding temperature were selected. The temperature was further specified by taking the temperature of the best fit and fitting again from -50 to +50 K in 1 K steps with respect to the temperature of the best fit. From these new fits, the temperature of the best fit was selected as the thermal radiation temperature.

4 Results and discussion

An example of the time evolution of Ca I line at 504.16 nm, Li I line at 670.78 nm, and CaF band centered around 535 nm have been presented in Fig. 1 with seven spectra taken from various instances. Spectrum 1 has been taken before the arc is switched on, displaying only the heat radiation from the molten bath. Planck's law fit to the spectrum 1 yields 1383 K for the temperature. Spectrum 2 is from the electric arc, where the atomic emissions are clearly seen and the CaF emissions are strongly self-reversed especially around 535 and 605 nm. Spectra 3 and 4 represent two close instances, where the arc is seen poorly or not at all, respectively. The intensity of the atomic optical emissions from the slag components is much lower than in spectrum 2, whereas only alkali and molecular emissions from CaO and CaF can be seen in spectrum 4. Spectra 5 and 6 are from a longer time period during which the arc's optical emissions are seen, showing how the arc spectra change from one instance to another. At spectrum 7, the arc has been switched off and a slag sample is taken

from the molten bath. This spectrum is similar to spectrum 4. At the sampling instances, Li I intensity tends to increase sharply. This can be seen in Fig. 1 a) at time 1300, where the relative intensity of Li I increases to around 0.2. The slag sampling spectrum has been verified on-site during the slag sampling process by the authors. The sampling is associated with flames and splatters occurring due to probe material reacting with the melt, which is likely the cause of the excitations.

The CaF and CaO optical emissions in the slag sampling spectrum 7, and most probably also spectrum 4, originate from the glowing slag surface. These molecular band structures are easily identified when the arc is not seen or it is switched off. However, when the arc is seen, the molecular optical emissions of CaF are usually strongly self-reversed and the CaO bands blend in with the other optical emissions. The self-reversed CaF has been marked in spectrum 2 of Fig. 1 b).

As can be seen from the spectra of Fig. 1 b), the full-widths at half maximum (FWHM) of the atomic emission lines are very broad, averaging between 1.5 and 2.0 nm. The main cause for this is that the measurement head sees frequently the reflections of the electric arcs and molten bath. Several Mg I, Fe I, Ca I, and Ca II lines have been marked on the spectrum 2 of Fig. 1 b). It should be mentioned that a single arrow in Fig. 1 b) may refer to several atomic emission lines, since there are e.g. three Mg I emission lines located at 516.73, 517.27, and 518.36 nm. These emission lines have merged together, which means that a convolution of multiple fit functions has to be used to distinguish the individual emission lines. The FWHM values were so broad that a comprehensive study of atomic emission lines was not performed due to significant overlapping with neighboring lines. Thus, the analysis focuses on the molecular optical emissions from CaO and CaF.

The spectra for the analysis were selected by locating a timestamp for the XRF result and selecting the nearest relevant spectra before this timestamp. However, not all cases had arc or molecular band spectra as near to the slag sampling as in Fig. 1. Cases with molecular band spectra and arc spectra ranged from 10 to 41 min before the XRF time stamp. If the spectra fulfilled the criteria set for the thermal radiation temperature and had enough of consequent spectra, they could be used in the composition analysis. Consequently, information on the slag composition could be gained 10 to 41 min before the XRF analysis for these cases.

Casting spout may provide a convenient view into the furnace, allowing simple equipment installation and maintenance. However, if the height of the molten bath or the lengths of the arcs vary a lot from heat to heat, the spectra may occasionally be very faint and distorted. Due to this, spectra from roughly half of the heats did not qualify for the slag composition evaluation analysis. In order to avoid these issues in an industrial application, the positioning of the OES equipment has to be carefully planned prior to the campaign. An immediate improvement in the future scenarios would be to relocate the OES measurement equipment to a position from which there is a better direct view into the arcs and molten bath, such as the furnace roof or outside the furnace at a position with a better angle towards the arcs. Additionally, adjusting the view-cone at which light is gathered could allow seeing the arcs despite the changing arc position and length.

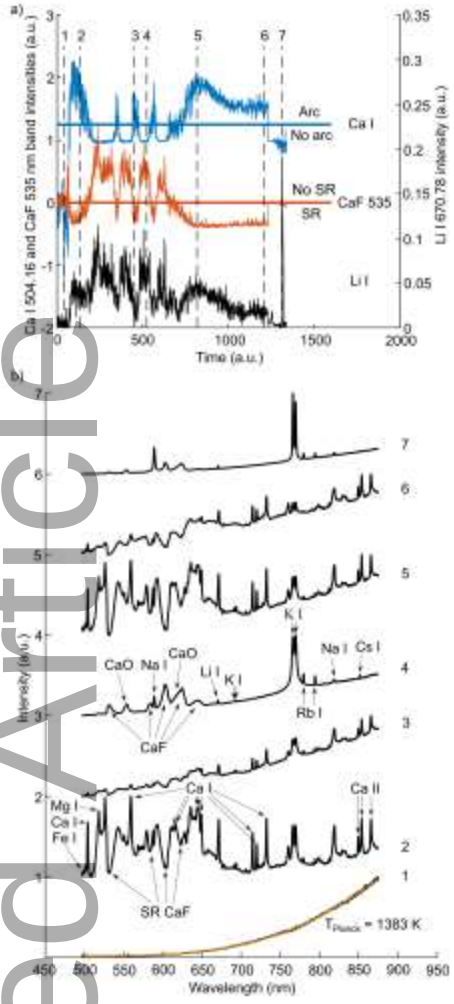

Figure 1: a) Time evolution of Ca I line at 504.16 nm, Li I line at 670.78 nm, and CaF band centered around 535 nm, and b) example spectra from time instances 1-7 in a). The spectra have been normalized, a y-axis offset has been applied to the spectra from 2 to 7, and the intensities of Ca I, Li I, and CaF 535 band are relative to the background radiation. The horizontal line across the Ca I depicts whether or not the arc with atomic optical emissions from the slag components is seen or not, whereas the horizontal line across the CaF 535 depicts if the CaF emission is self-reversed or not. Planck's law fit (solid line) to the thermal radiation of spectrum 1 yields 1383 K. Slag sampling is at spectrum 7.

4.1 Spectra from the molten bath and poorly visible arc

In this study, it was found out that molecular optical emissions from CaF and CaO can be observed from the molten bath even when the arc is switched off. The molecular emissions of CaF originate from the transitions $B\,^2\Sigma^+ \rightarrow X\,^2\Sigma^+$ and $A\,^2\Pi \rightarrow X\,^2\Sigma^+$ [21, 22, 23, 24, 25]. Optical emissions from CaO, on the other hand, arise from transitions involving several energy states [21]. These molecular emissions are present also in the arc spectra, but they are overlapping with several atomic emission lines and CaF emission bands tend to be strongly self-reversed.

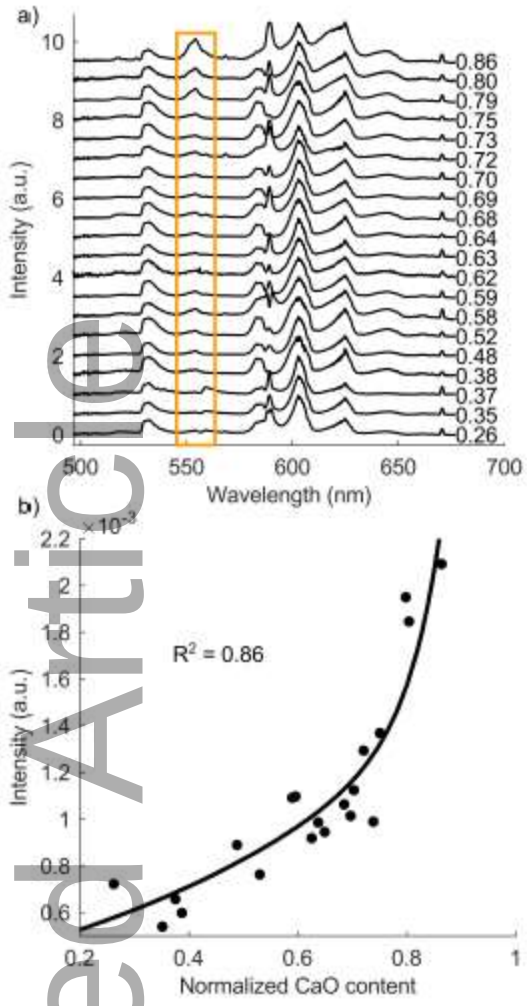

Figure 2: a) 20 spectra with increasing CaO content of slag and b) relation between the CaO band intensity around 550 nm and the CaO content of the slag. The CaO content has been indicated to the right of each spectrum in a) and intensities in b) are relative to the spectrum range from 500 to 680 nm. The temperature range of the thermal radiation is from 2000 to 2100 K. The total number of slag samples fulfilling these requirements was 23, but 3 cases had to be excluded due to strong mixing with the arc or poor visibility into the furnace. The intensities of b) are means over the last 60 s.

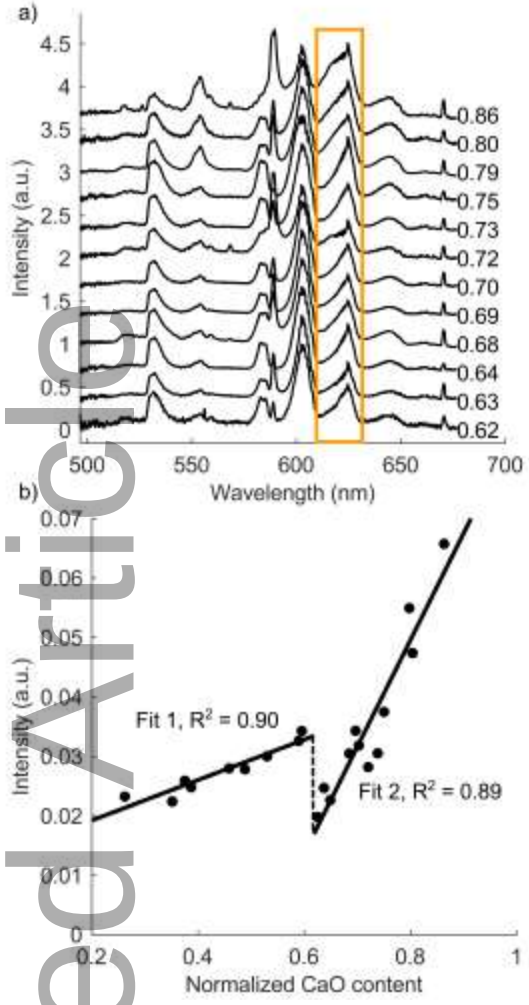

Figure 3: a) 12 spectra with increasing CaO content of slag and b) relation between the CaO band intensity around 625 nm and the CaO content of the slag. The CaO content has been indicated to the right of each spectrum in a) and intensities in b) are relative to the spectrum range from 500 to 680 nm. The temperature range of the thermal radiation is from 2000 to 2100 K. The total number of slag samples fulfilling these requirements was 24, but 3 cases had to be excluded due to strong mixing with the arc or poor visibility into the furnace. The intensities of b) are means over the last 60 s.

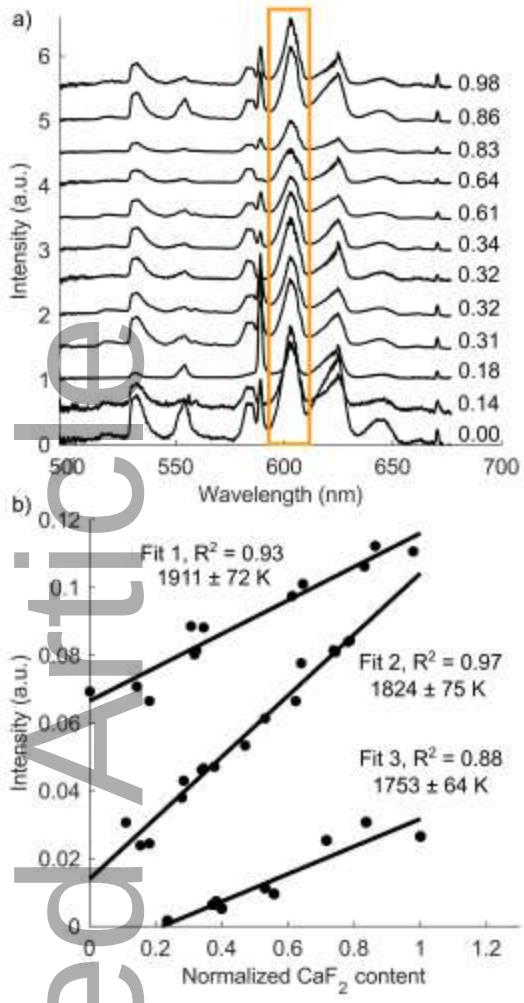

Figure 4: a) 12 spectra with increasing CaF_2 content of slag and b) relations between the CaF band intensity around 605 nm and the CaF_2 content of the slag separated with thermal radiation temperature. The CaF_2 content has been indicated to the right of each spectrum in a) and intensities in b) are relative to the spectrum range from 500 to 680 nm. The spectra of a) are from Fit 1 in b). The temperature range of the thermal radiation is from 1600 to 2000 K. The total number of slag samples fulfilling these requirements was 52, but 15 cases had to be excluded due to strong mixing with the arc or poor visibility into the furnace. The intensities of b) are means over the last 60 s.

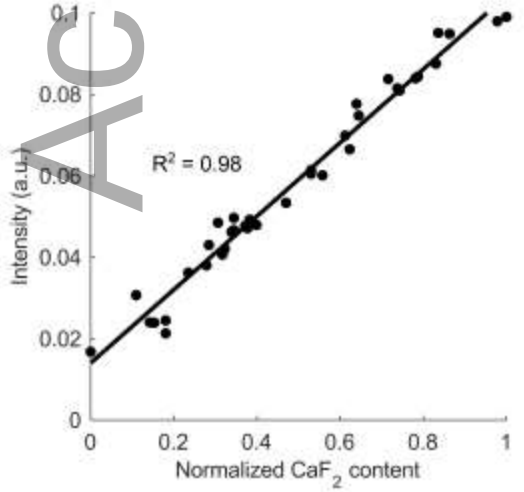

Figure 5: Aligned Fits 1-3 from Fig. 3 derived with the linear fit functions. The fits have been

aligned with respect to Fit 2. The total amount of heats in the fit is 37.

Fig. 2 a) represents 20 spectra with increasing CaO content and b) relation between normalized CaO content of the slag and the mean intensity of the band near 550 nm over the last 60 s of the observed spectra. The relative intensity of the CaO band increases significantly for the four spectra with the highest amount of CaO in the slag. The thermal radiation temperatures were limited to the range between 2000 and 2100 K for Fig. 2 b). If temperatures below or above this range were included, the relation dissipated. Other temperature ranges did not show a relation between relative CaO intensity and CaO in slag. This band was observed to be promising for slag composition analysis purposes because there are no other significant optical emissions near it when the optical emissions from the arc are not seen. The CaO contents that can be derived from the fit of Fig. 2 have a mean difference of 2.19 % with a standard deviation of 1.92 %. The mean difference is with respect to the XRF composition value, and the standard deviation describes how much these differences vary.

CaO has another wide emission band structure between 590 and 650 nm, with the highest intensities around 625 nm. This region does, however, overlap with the CaF optical emissions. Fig. 3 a) represents 12 spectra with increasing CaO content and b) relations between normalized CaO content of the slag and the mean intensity of the Fit 2 of Fig 3 b) near 625 nm over the last 60 s of the observed spectra. There is a drop in the relative intensities around 0.62 CaO content of the slag, after which the relative intensity of the CaO band increases steeply. This behavior arises most probably from the overlapping with the CaF emissions, which complicate the fitting of the bands.

Fig. 4 a) represents 12 spectra with increasing CaF_2 content and b) relations between normalized CaF_2 content of the slag and the mean intensity of the band near 605 nm over the last 60 s of the observed spectra. The main difference to the definition of CaO bands is that the temperature range was between 1600 and 2000 K for the CaF bands. As can be seen from Fig. 4 b), the relations between the relative spectrum intensities and CaF_2 content of the slag are separated by the thermal radiation temperatures. The cases of Fit 1 are observed before, during, or after when the arc is on but not directly in the view-cone, Fit 2 when the arc has been off for a longer time period, and Fit 3 when the spectra have lower overall intensity and the bands are observed for only several seconds. The thermal radiation temperatures are relatively high for a molten slag surface, indicating that the temperature is high due to the recent presence of the arc. Furthermore, the melting points of CaO and CaF_2 are near 2300 K and 1150 K, respectively. The differences in the CaO and CaF_2 thermal radiation temperatures ranges could well be caused by the high difference in the melting properties of these two components. Since the data points of Fig. 4 b) can be attributed to different correlation fits based on the known process instances from which the spectra were taken, the fits can be aligned with one another based on this. This has been done in Fig. 5. The CaF_2 contents that can be derived from the fit of Fig. 5 have a mean difference of 0.59 % with a standard deviation of 0.46 %. The mean difference is with respect to the XRF composition value, and the standard deviation describes how much these differences vary. With the fits of Figures 2, 3, and 5, the CaO and CaF_2 content of the slag can be analyzed from the molten bath spectra.

4.2 Spectra from the arc

All of the CaF optical emissions are self-reversed for most of the arc spectra. CaO emissions, on the other hand, are obscured by atomic emission lines and overlap with the self-reversed CaF bands. The arc spectra have an abundance of atomic emission lines from various slag components, as can be seen in spectra 2, 3, 5, and 6 of Fig. 1 b). Due to the very high FWHM values of the atomic emission lines and obscured molecular optical emissions from CaO, the arc spectrum analysis focuses on the CaF bands.

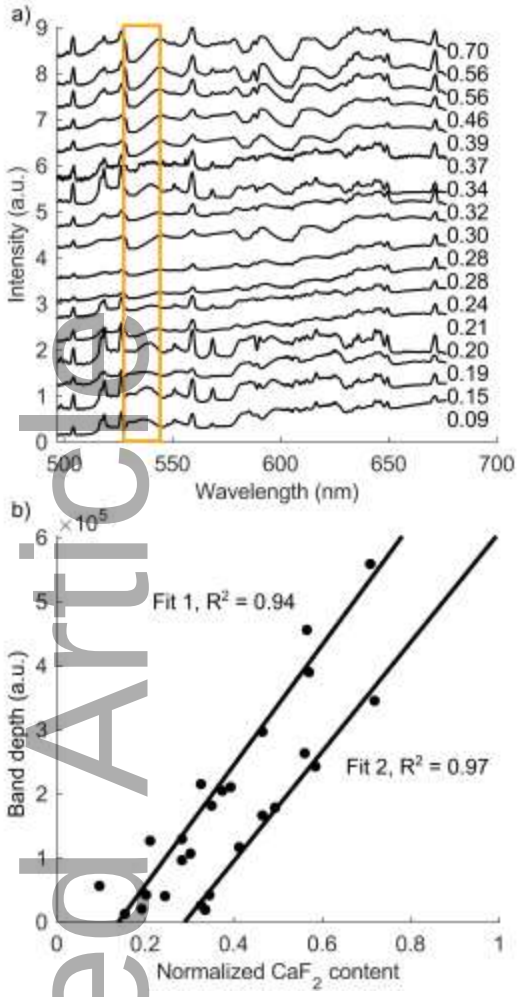

Figure 6: a) 17 spectra with increasing CaF_2 content of slag and b) relations between the CaF band intensity around 535 nm and the CaF_2 content of the slag. The CaF_2 content has been indicated to the right of each spectrum in a). The spectra of a) are from Fit 1 in b). The intensities of b) are means over the last 2 arc spectra.

Fig. 6 a) represents 17 arc spectra with increasing CaF_2 content and b) relations between normalized CaF_2 content of the slag and the depth of the self-reversed CaF emission band around 535 nm. The self-reversal begins to be very noticeable above 0.30 of normalized CaF_2 content. Fit 1 is typically observed when the arc has been on for a longer time period, and Fit 2 is when the arc has been on for short time periods. As can be seen from the spectra, the atomic emission lines are so wide that some of them form clustered bumps to the spectra instead of separated lines. Thus, the casting spout is not ideal for OES measurements that would require high-accuracy fitting of atomic emission line intensities and preferably low FWHM values. However, there are several Ca I and Ca II emission lines above 700 nm that are so far apart from one another that they can be resolved as individual lines.

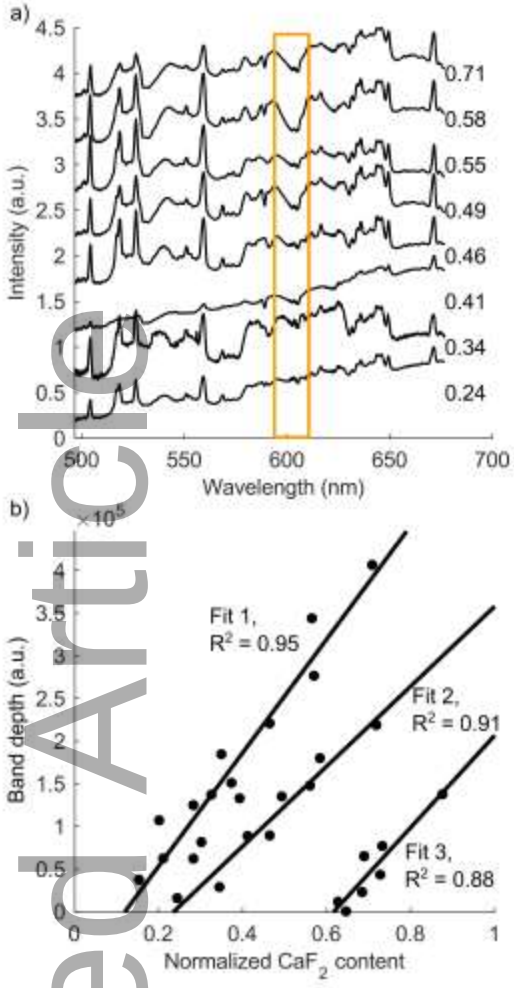

Figure 7: a) 8 spectra with increasing CaF_2 content of slag and b) relations between the CaF band intensity around 605 nm and the CaF_2 content of the slag. The CaF_2 content has been indicated to the right of each spectrum in a). The spectra of a) are from Fit 2 in b). The intensities of b) are means over the last 2 arc spectra.

Similar to Fig. 6, Fig. 7 a) represents 8 arc spectra with increasing CaF_2 content and b) relations between normalized CaF_2 content of the slag and the depth of the self-reversed CaF emission band around 605 nm. The cases of Fig. 7 are the same as in Fig. 6 for the most part, but additional slag samples could be attributed to the CaF_2 content of the slag as depicted in Fit 3 of Fig. 7. The cases of Fit 1 are typically observed when the arc has been on for long, Fit 2 when the arc has been switched on and off and has not been directly in the view-cone, and Fit 3 when the arc spectra have had lower intensity or the arc has been obscured.

The self-reversal of these CaF bands has a significant effect on the spectra around the central wavelength of the bands and selecting optical emission lines near these bands should be avoided. However, these bands are a clear indicator of the presence of fluorine in the slag as the optical emissions from CaF can originate both from the CaF_2 in the slag or recombination of Ca and F in the arc plasma. Hence, the fluorine content of slag could also be addressed with the CaF bands even though the slag would not specifically contain CaF_2. As a halogen, fluorine emission lines can be hard to detect due to high excitation energy, and thus the CaF emission bands could be more favorable to quantify the fluorine content.

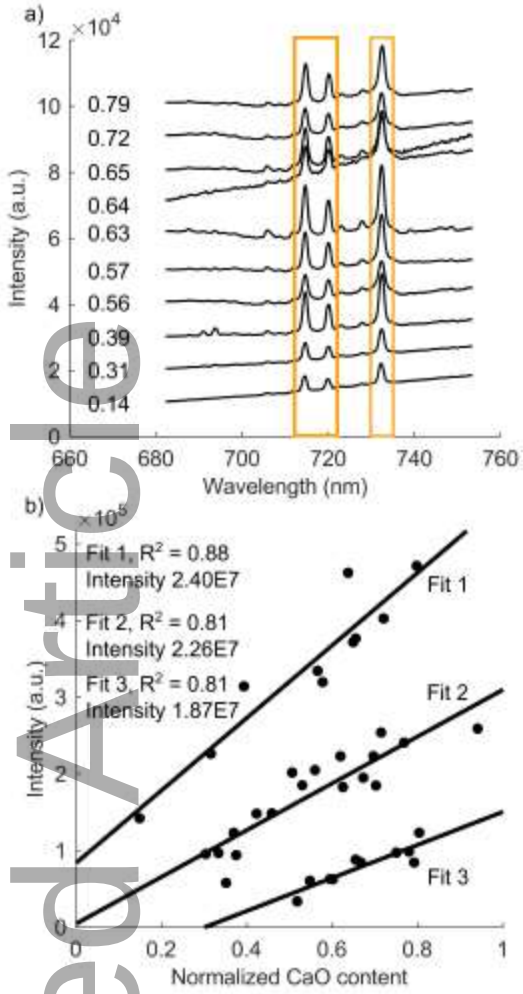

Figure 8: a) 10 spectra with increasing CaO content of slag and b) relations between the summed intensity of the three Ca I lines at 714.82, 720.22, and 732.62 nm and the CaO content of the slag. The CaO content has been indicated to the left of each spectrum in a). The spectra of a) are from Fit 1 in b). The intensities of b) are means over the last 2 arc spectra. The intensity values ranging from 1.87E7 to 2.40E7 in b) are means over the whole spectrum intensity.

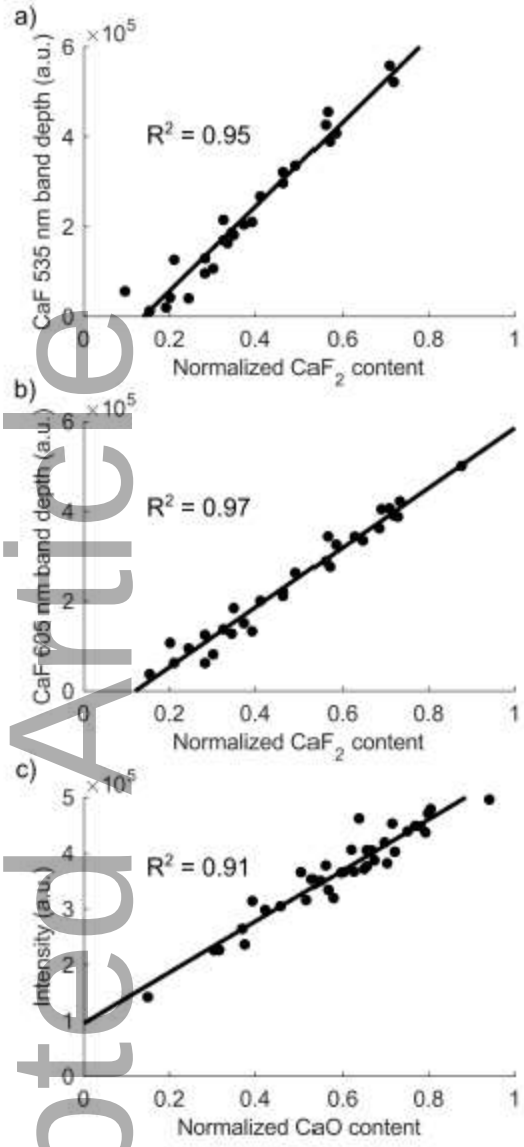

Figure 9: Aligned fits from a) Fig. 5, b) Fig. 6, and c) Fig. 7. The total amount of heats in the fits are a) 26, b) 29, and c) 39.

There are three Ca I atomic emission lines above 700 nm that are several nanometers apart from one another, allowing reliable determination of line intensities despite the high FWHM values. These three emission lines are listed in the NIST Atomic Spectra Database [18], but they do not have line-specific data available. Fig. 8 a) shows these Ca I emission lines and b) relations between the summed intensity of the Ca I lines within the wavelength range between 712 and 735 nm. The last arc spectra were 11 to 41 min before the XRF timestamp. The mean intensity of the last two arc spectra had the best relation to the CaO content of the slag, regardless of how far away the spectra were from the XRF timestamps.

The Fits 1, 2, and 3 of Fig. 8 represent similar cases to the ones in Fig. 7. Furthermore, the Fits of Fig. 8 b) are separated by differences in the overall spectrum intensity. The visibility of the arc has a key role in these relations. This can be evaluated from the spectra by observing both the overall intensity of the spectra and the intensities of individual atomic emission lines from the arc. Subtracting the thermal background caused by the molten bath and the arc itself is one way to assess these issues.

Similar to Fig. 5, the fits from Figs. 6 to 8 have been aligned in Fig. 9. For these data sets, For these data sets, the CaF content is predicted with a mean difference of 0.58 % and standard deviation of 0.50 % with a), and a mean difference of 0.61 % and standard deviation of 0.56 % with b). The

CaO content is predicted with a mean difference of 0.67 % and a standard deviation of 0.56 % with c). The mean difference is with respect to the XRF composition value, and the standard deviation describes how much these differences vary. For the arc spectra, the fits of Fig. 8 can be used to analyze the CaO and CaF_2 content of the slag.

The division of the optical emissions to different correlations in Figs. 6 - 8 means that the optical emissions from the slag components correlate differently to the slag composition depending on the process instance. Consequently, this suggests that these differences arise from the varying properties of the plasma or the evaporation of material during the heat. The arc properties have been reported to fluctuate in a pilot-scale AC EAF study, including also varying plasma temperature and electron density [14]. Additionally, the properties of the plasma have been observed to fluctuate also in industrial EAF [16]. Due to the uncertainty related to the convolution of several overlapping high-FWHM emission lines, plasma diagnostics have not been performed in this study. Determining the properties of the plasma and molten bath over the course of several heats with respect to the electrical input of the furnace would be a beneficial research topic for a future measurement campaign, where the OES equipment has been relocated for a clear view into the furnace.

5 Conclusion

In this study, the CaO and CaF_2 content of slag has been evaluated with optical emission spectra measured through the casting spout. Molecular optical emissions of CaO and CaF could be attributed to the CaO and CaF_2 content of the slag. High-intensity molecular optical emissions were clearly observed from the molten bath, whereas the CaO bands were obscured by atomic optical emissions lines and CaF bands were strongly self-revered in the arc spectra.

The relations between the OES and XRF data were separated into different correlations depending on the instance when the spectra were observed, the temperature of the molten bath, and the overall intensity of the spectra. In general, the visibility of the arc and how long the arc had been switched on had a significant influence on these correlations. Several optical emissions from CaO, CaF, and Ca I were correlated to the XRF slag composition analyses based on the spectra that were observed within the last 60 s of each spectrum type, i.e. spectra from the molten bath or the arc. The mean over the last few spectra and the last 60 s were used for the arc and the molten bath spectra, respectively. The relevant spectra were from 10 to 41 minutes before the XRF analysis time stamp. Since OES provides spectra in real-time, it has the potential to be used to assess how the slag composition changes during the melting. However, the erratic behavior of the electric arcs together with the electrical input of the furnace has to be considered and taken into account in the analysis.

As a measurement location, casting spout has both advantages and disadvantages. If the spout provides a view into the furnace, it can be used as a safe and easy location for the spectrometer's measurement head. However, since the reflections of the arc and molten bath are sometimes seen instead of a direct view to the arc, the spectra may have disturbances, such as wavelength shift and broadening of emission lines. In this study, the molecular optical emissions were easily identified from the spectra, but atomic emission lines overlapped with one another significantly if they were not several nanometers apart. In order to improve the spectrum quality, the OES equipment could be relocated to the furnace roof or to a different place outside the furnace with a better view into the furnace. Alternatively, several spectrometers that have been aimed at different locations in the furnace could be used.

Acknowledgements

We acknowledge the support of the Research Fund for Coal and Steel under grant agreement No. 709923, Academy of Finland for Genome of Steel grant No. 311934, Business Finland for grant No. 4478/31/2019.

Conflict of interest

The authors declare that they have no conflict of interest.

References

[1] S. Manocha, F. Ponchon, *Metals* **2018**, *8*, 9.

[2] C. Behera, U. K. Mohanty, *ISIJ Int.* **2001**, *41* 834.

[3] K. Y. Ko, J. H. Park, *ISIJ Int.* **2013**, *53* 958.

[4] J. H. Park, D. J. Min, H. S. Song, *Metall. Mater. Trans. B* **2002**, *33* 723.

[5] J. H. Park, K. Y. Ko, T. S. Kim, *Metall. Mater. Trans. B* **2014**, *46* 741.

[6] F. Shahbazian, *Scand. J. Metall.* **2008**, *30* 302.

[7] J. G. L. Wu, D. Sichen, *Metall. Mater. Trans. B* **2011**, *42* 928.

[8] E. Andersson, D. Sichen, *Steel Res. Int.* **2009**, *80*, 8 544.

[9] A. Picon, A. Vicente, S. Rodriguez-Vaamonde, J. Armentia, J. A. Arteche, I. Macaya, *IEEE Trans. Ind. Inform.* **2018**, *14*, 8 3506.

[10] M. Aula, A. Mäkinen, T. Fabritius, *Appl. Spectrosc.* **2014**, *68*, 1 26.

[11] M. Aula, T. Demus, T. Echterhof, M. Huttula, T. Fabritius, *ISIJ Int.* **2017**, *57* 478.

[12] M. Aula, A. Leppänen, J. Roininen, E.-P. Heikkinen, K. Vallo, T. Fabritius, M. Huttula, *Metall. Mater. Trans. B* **2014**, *45* 839.

[13] M. Aula, A. Mäkinen, A. Leppäanen, M. Huttula, T. Fabritius, *ISIJ Int.* **2015**, *55*, 8 1702.

[14] H. Pauna, T. Willms, M. Aula, T. Echterhof, M. Huttula, T. Fabritius, *Plasma Res. Express* **2019**, *1*, 3 035007.

[15] H. Pauna, M. Aula, J. Seehausen, J.-S. Klung, M. Huttula, T. Fabritius, *ISIJ Int.* **2020**,

60 1985.

[16] H. Pauna, M. Aula, J. Seehausen, J.-S. Klung, M. Huttula, T. Fabritius, *Steel Res. Int.* **2020**, *91*, 11 2000051.

[17] H. Pauna, T. Willms, M. Aula, T. Echterhof, M. Huttula, T. Fabritius, *Plasma Res. Express* **2021**, *3*, 2 025008.

[18] A. Kramida, Y. Ralchenko, J. Reader, NIST ASD Team, Nist atomic spectra database, URL https://doi.org/10.18434/T4W30F , Accessed: 08, 2021.

[19] C. Aragón, J. A. Aguilera, *Spectrochim. Acta B* **2008**, *63* 893.

[20] R. D. Cowan, G. H. Dieke, *Rev. Mod. Phys.* **1948**, *20* 418.

[21] A. A. Bol'shakov, X. Mao, R. E. Russo, *J. Anal. At. Spectrom.* **2017**, *32* 657.

[22] M. Gaft, L. Nagli, N. Eliezer, Y. Groisman, O. Forni, *Spectrochim. Acta B* **2014**, *98* 39.

[23] C. Alvarez-Llamas, J. Pisonero, N. Bordel, *Spectrochim. Acta B* **2016**, *123* 157.

[24] C. Alvarez-Llamas, J. Pisonero, N. Bordel, *J. Anal. At. Spectrom.* **2017**, *32* 162.

[25] D. S. Vogt, S. Schröder, K. Rammelkamp, P. Hansen, S. Kubitza, H.-W. Hübers, *Icarus* **2020**, *335* 113393.

In-situ optical emission spectroscopy is used to study the light emitted by the arc and the molten bath through the ladle furnace's casting spout. With this method that is viable also for on-line analysis, molecular optical emissions from CaO and CaF together with atomic emissions are used to derive correlations between the spectra and the slag's CaF_2 and CaO content.